Targeted therapy for triple-negative breast cancer
McLaughlin, R.P.

Citation

McLaughlin, R. P. (2018, December 13). *Targeted therapy for triple-negative breast cancer*. Retrieved from https://hdl.handle.net/1887/68194

Cover Page

Universiteit Leiden

Leiden University Repository

The handle http://hdl.handle.net/1887/68194 holds various files of this Leiden University dissertation.

Author: McLaughlin, R.P.
Title: Targeted therapy for triple-negative breast cancer
Issue Date: 2018-12-13

Chapter 5

The synergistic effect of combined P-TEFb and EGFR inhibition on triple-negative breast cancer

Ronan P. McLaughlin[1], Jichao He[1], Jessica Karuntu[1], Vera van der Noord[1], John W.M. Martens[2], John A. Foekens[2], Marcel Smid[2], Solomon Tadesse[3], Yi Long[3], Sarah Al Haj Diab[3], Shudong Wang[3], Yinghui Zhang[1], Bob van de Water[1]

[1]Division of Drug Discovery and Safety, Leiden Academic Centre for Drug Research, Leiden University, 2300 RA Leiden, The Netherlands.

[2]Department of Medical Oncology and Cancer Genomic Netherlands, Erasmus MC Cancer Institute, Erasmus University Medical Center, 3000 CA Rotterdam, The Netherlands.

[3]Centre for Drug Discovery and Development, School of Pharmacy and Medical Sciences, University of South Australia Cancer Research Institute, Adelaide, South Australia, 5001, Australia.

This chapter is based on a manuscript in preparation

ABSTRACT

There is a lack of effective targeted therapies against triple negative breast cancer (TNBC). Despite expressing EGFR, TNBC is generally resistant to EGFR-tyrosine kinase inhibitors (EGFR-TKIs). Increasing evidence suggests multiple cancers depend upon aberrant transcriptional programs controlled by the positive transcription elongation factor b (P-TEFb) complex. Consequently, we explored the sensitivity of TNBC cells to disruption of P-TEFb-mediated transcriptional regulation and its potential to overcome resistance to EGFR-TKIs. Here we show that combining CDK9 inhibitors I-73 and Y3-21 with EGFR-TKIs lapatinib and gefitinib, abolishes the resistance of TNBC cells to these agents. Co-treatment resulted in strong anti-proliferative synergistic responses associated with cell cycle arrest, depletion of anti-apoptotic protein MCL-1, and induction of apoptosis. Transcriptomic profiling revealed that targeting EGFR and CDK9 simultaneously, potentiated the inhibitory effect of CDK9 inhibition on gene expression, down-regulating genes linked to stem cell pluripotency, TGF-β signalling, and cell cycle progression, whilst blocking growth factor-mediated networks such as downstream MAPK/MEK signalling. Co-inhibition of EGFR and CDK9 signalling preferentially obstructed the function of multiple transcription factors, the expression of a number of which was associated with a significantly shorter metastasis-free survival in TNBC patients. In summary, interruption of P-TEFb/CDK9-mediated transcription abrogates the resistance of TNBC cells to EGFR inhibition, thereby preventing TNBC cell proliferation, emphasising the potential of combining such targeted therapies in treating drug-resistant TNBC.

INTRODUCTION

Triple-negative breast cancer (TNBC) is a virulent form of breast cancer associated with a dismal prognosis and metastatic propensity when compared to hormone receptor- and HER2-positive breast cancer[1–3]. TNBC displays remarkable genetic heterogeneity, precluding the identification of bona fide oncogenic drivers amenable to pharmacological manipulation, thus preventing the development of effective targeted therapies[4–7]. However, emerging evidence suggests that targeting key transcriptional regulators, such as positive transcription elongation factor b (P-TEFb), which act as downstream convergence points for signals transduced via receptor tyrosine kinase (RTK)-mediated signalling, may represent a strategy to identify novel therapies and synergistic combinations with enhanced efficacy for TNBC as well as other cancers[8,9]. P-TEFb is a complex composed of catalytic cyclin-dependent kinase 9 (CDK9) and its partner Cyclin T1 which phosphorylates the C-terminal domain (CTD) of RNA Polymerase II (RNAPII) at Ser2 to allow productive mRNA elongation[10–13]. The activity of P-TEFb is partly controlled by bromodomain-containing protein 4 (BRD4) which, in the presence of Hexim1, is essential for the formation of the complex, its binding to the CTD of RNA II and its activation, by promoting the dissociation of negative transcription elongation factors such as 7SK snRNA[11,13,14].

Multiple research groups have elaborately investigated the potential of disrupting CDK7 or P-TEFb/CDK9 transcriptional function in various malignancies, including ovarian cancer, neuroblastoma, acute myeloid leukaemia (AML) and T-cell leukaemias[15–18]. The identification of super-enhancer associated genes dependent upon CDK7-mediated transcription in EGFR-tyrosine kinase inhibitor (EGFR-TKI)-resistant TNBC cells by means of CRISPR-Cas screening suggested that RTK-

targeted therapies could be augmented by combining them with inhibitors of transcription[19]. Moreover, in response to RTK-targeted therapies, cancers are capable of reprogramming their signalling circuitry to avoid RTK-targeted therapy-induced apoptosis[20,21]. This results in the enhanced expression of alternative RTKs which funnel growth factor-regulated signal transduction, thereby diminishing the efficacy of RTK-targeted therapies which seek to exploit the addiction of cancer cells to oncogenic growth factor-mediated signalling[20,22]. Recent data show that in TNBC tumours treated with MEK1/2 inhibitor trametinib, disruption of P-TEFb function mitigates this adaptive bypass mechanism[9]. By preventing enhancer remodelling-mediated up-regulation of alternative RTKs FGFR2, PDGRB and DDR1, through which MEK1/2 activation can continue unabated, an enhanced response to trametinib was observed[9]. Also, preventing activation of P-TEFb by use of BRD4 inhibitor I-BET151 profoundly suppressed TNBC xenograft growth, whilst silencing of CDK9 attenuated trametinib-mediated enhanced expression of DDR1 and PDGFRB and downstream ERK1/2 activation in TNBC cell lines *in vitro*[9]. At the molecular level, co-treatment with P-TEFb/CDK9 inhibitors or BRD4 inhibitors precluded recruitment of RNAPII to active gene promoters involved in the up-regulation of PDGFR and FGFR[9].

Nonetheless, information on the effectiveness of combining EGFR-TKIs with agents that disrupt P-TEFb/CDK9 function in EGFR-TKI-resistant TNBCs is unavailable. EGFR overexpression and amplification, as well as reliance on EGFR-regulated signal transduction are common in TNBC tumours and higher expression of EGFR confers a poorer prognosis to patients[23–28]. Considering the aforementioned extensive pre-clinical testing of BRD4 inhibitors in combination with RTK- and MEK-

targeted therapies, there is a clear justification for combined targeting of RTK-mediated signaling and P-TEFb-regulated transcription in TNBC[29,30]. Eradicating the proclivity of drug-resistant TNBC cells for transcriptional plasticity in response to targeted therapy, may enhance the response to RTK-targeted agents such as EGFR-TKIs which have yet to demonstrate appreciable clinical benefit in TNBC[23,28,31].

Here we investigated the impact of combining EGFR-TKIs and P-TEFb/CDK9 inhibitors in a panel of TNBC cell lines, the majority of which are insensitive to EGFR-TKIs[19]. Our results demonstrate that combining potent P-TEFb/CDK9 inhibitors with clinically approved EGFR-TKIs synergistically inhibits the proliferation of TNBC cells, induces apoptosis, and down-regulates important components of the transcriptional machinery critical to TNBC cell survival.

MATERIALS & METHODS

Cell Culture

TNBC cell lines used were representative for different TNBC subtypes[32], including basal-like 1 (BL1) HCC38, HCC1143, HCC1937 and MDA-MB-468; basal-like 2 (BL2) HCC70, HCC1806 and SUM149PT,; mesenchymal (M) BT549 and Hs578T; mesenchymal stem-like (MSL) MDA-MB-157, MDA-MB-231, MDA-MB-436 and SUM159PT; luminal androgen receptor (LAR) MDA-MB-453; and unclassified SKBR7, SUM52PE, SUM229PE and SUM1315MO2. All TNBC cell lines were maintained in RPMI-1640 medium (*Gibco, ThermoFisher Scientific*) supplemented with 10% FBS (*Thermo Fisher Scientific; 10270106*) and 25IU/ml Penicillin and 25µg/ml Streptomycin (*ThermoFisher Scientific*; *15070-063*). Cells were cultured in a humidified incubator at 37°C, 5% CO_2.

Kinase inhibitor combination screen

CDK9 inhibitors I-73[33] and the new generation inhibitor Y3-21 were acquired from the Centre for Drug Discovery and Development, University of South Australia. EGFR inhibitors lapatinib (S1028) and gefitinib (S1025), and BRD4 inhibitor JQ1 (S7110) were purchased from Selleckchem®. Cells were seeded at the appropriate densities (90 µl/well) in 2x 96-w plates (for SRB; *Greiner; 655162*) and 2x 96-w µCLEAR plates (for imaging; *Greiner; 655090*) and incubated overnight at 37°C, 5% CO_2. Cells were subsequently treated with a dose range of inhibitors (0.0316 µM – 3.16 µM), e.g. EGFR inhibitors lapatinib and gefitinib or BRD4 inhibitor JQ1, combined with two single doses of I-73 (0.1 µM or 0.316 µM) or Y3-21 (0.0316 µM or 0.1 µM). Cells were subsequently incubated at 37°C, 5% CO_2 for 96 hours, followed by proliferation assay.

Automated imaging of apoptosis

72 hours post-exposure to inhibitors and prior to sulphorhodamine B proliferation assay, cells were stained with 1:1000 Annexin-V (0.9 mg/ml) and 1:10,000 Hoechst 33258 (2 mg/ml) for 45 minutes at 37°C, 5% CO_2. Cells were subsequently imaged using BD Pathway 855 microscope (BD Biosciences). An image analysis pipeline was created in Cell Profiler involving segmentation based on Hoechst 33258 staining to identify the primary cell objects followed by secondary Annexin V-positive objects. Annexin V-positive cells were defined based on an intensity threshold. This threshold was set based on the negative (DMSO) and positive (doxorubicin) controls. For each image the sum of all nuclei and the sum of the Annexin V-positive cells was determined followed by calculation of the percentage of Annexin V-positive cells.

Sulphorhodamine B (SRB) proliferation assay

SRB Assay was performed as previously described after 96 hours' exposure to indicated inhibitors[34,35].

Western blotting

Cell lysates were harvested in RIPA lysis buffer with 1:100 protease inhibitor cocktail (Sigma; P8340). Cellular proteins were denatured in sample buffer containing 10% β-mercaptoethanol (Acros Organics 125472500). Equal amounts of proteins were subsequently loaded into polyacrylamide gels (7.5-15% depending on desired resolution), resolved using SDS-PAGE and subsequently transferred to PVDF membranes (Merck Chemicals; IPVH00010) overnight. PVDF membranes were then blocked with 5% bovine serum albumin (Sigma Aldrich A9647) in Tris-buffered saline containing 0.05% Tween20 and incubated overnight with the appropriate primary antibodies: phospho-CDK9 (T186; CST 2549), CDK9 (CST 2316), phospho-RNAPII (S2/5; CST 4735), RNAPII (CST 2629), BRD4 (Bethyl Laboratories A301-985A-M), BCL-xL (CST 2764), MCL1 (CST 5453), γ-H2AX (S139; CST 2577) and tubulin (Sigma Aldrich T-9026).

Cell cycle analysis

Cells were seeded in 6-well plates at the appropriate density. The following day cells were treated with drugs for 48 hours. Detached cells and attached cells were collected during trypsinisation and collected through centrifugation (1000 rpm, 5 minutes, 4°C). Pelleted cells were re-suspended in 200 μl ice-cold 1 mM EDTA in PBS and fixed by adding 800 μl ice-cold 100% ethanol (-20°C). Cells were washed by two wash steps in PBS (1000 rpm, 5 minutes, room temperature) and pellet was

re-suspended in 250 µl of 3 µM DAPI (Sigma Aldrich, 10236276001) in staining buffer (100 µM Tris pH 7.4, 150 mM NaCl, 1 mM $CaCl_2$ and 0.5 mM $MgCl_2$). After 15 minutes cells were filtered through 70 µm EASYstrainer filters followed by FACS Conto II analysis (BD Biosciences). Data were analysed using FlowJo V10.

RNA-sequencing

Hs578T cells were seeded into 6-well plates, in triplicate, at the appropriate density and allowed to attach overnight at 37°C, 5% CO_2. Lapatinib and I-73 solutions were prepared at 3.16 µM and 0.1 µM, respectively and cells were treated with each inhibitor separately or in combination, or DMSO as control for 6 hours. RNA was subsequently extracted using RNeasy Plus Mini Kit (QIAGEN *74136*) according to the manufacturer's instructions and stored at -80°C. Transcriptome RNA-Sequencing (RNA-Seq) was performed using Illumina high-throughput RNA sequencing. DNA libraries were prepared from the samples with the TruSeq Stranded mRNA Library Prep Kit. The DNA libraries were sequenced according to the Illumina TruSeq v3 protocol on an Illumina HiSeq2500 sequencer. Paired-end reads were generated of 100 base-pairs in length. Alignment was performed using the STAR aligner (version 2.4.2a) against the human GRCh38 reference genome. Marking duplicates, sorting and indexing were performed using Sambamba (version 0.6.6). Gene expression was quantified using the FeatureCounts software (version 1.4.6) based on the ENSEMBL gene annotation for GRCH38 (release 84). RNA-Seq data were normalised by TMM using EdgeR's normalisation-factor, followed by quantile normalisation and presented in Log2 fold change (Log2 FC) scales[36]. Genes with significant down- or up-regulation (Log2 FC ≥ |0.68|) under indicated conditions were analysed by web-based functional analysis tool Ingenuity Pathway Analysis (IPA).

Clinical evaluation of candidate genes

The clinical relevance of synergy-related genes identified by transcriptomic profiling was evaluated using in-house and publicly available gene expression data of lymph node-negative (LNN) primary breast cancer patients who did not receive adjuvant or neo-adjuvant systemic therapy, as well as available metastasis-free survival (MFS) data, thereby generating a cohort of 867 patients. 625 of these were ER+, whilst 242 were ER-. Of the 242 ER-patients, 142 were classified as TNBC. Data were gathered from Gene Expression Omnibus (http://www.ncbi.nlm.nih,gov/geo/) entries GSE2034, GSE5327, GSE2990, GE7390 and GSE11121, with all data available on Affymetrix U133A chip. Raw.cel files were processed using fRMA parameters (median polish) after which batch effects were corrected using ComBat[37,38].

Data analysis & statistics

50% proliferation inhibition (IC50) values were derived from GraphPad Prism 7.0 using nonlinear regression fitting. The synergistic effect of drug combinations was analysed by combination index calculations (CI)[39–41], using the formula "CI = D1/D1x + D2/D2x, in which D1 and D2 are the respective combination doses of drug 1 and drug 2 that yield an effect of 50% of proliferation inhibition, and D1x and D2x are the corresponding single doses for drug 1 and drug 2 that result in 50% of proliferation inhibition (i.e. IC50). Two-way ANOVA with Tukey's multiple comparison test was used to assess impact of drug treatment on cell cycle distribution. P-values < 0.05 were considered statistically significant.

RESULTS

Co-targeting CDK9 and BRD4 synergistically inhibits proliferation and blocks P-TEFb-mediated signal transduction in TNBC cells

Since BRD4, is a positive regulator of P-TEFb[11], firstly we examined the expression of BRD family members in 116 TNBC patient tumours using available TCGA datasets (Supplementary Figure S1A). BRD2 and BRD4 were particularly highly expressed across all TNBC tumours analysed. To evaluate the utility and validity of our TNBC cell line panel, we compared the expression of BRD members in 20 in-house TNBC cell lines (Supplementary Figure S1B). The expression of BRD members in the cell line panel was largely comparable with their expression in the tumours, suggesting that the cell lines are useful models for testing sensitivity to BET inhibitors. Again, BRD2 and BRD4 were amongst the most highly expressed BRD members in the TNBC cell lines.

We have previously demonstrated that TNBC cells are vulnerable to disruption of P-TEFb-mediated transcriptional regulation by inhibiting CDK9 kinase activity. We therefore sought to address whether TNBC cells are also sensitive to inhibition of BRD4, the recruiter of the P-TEFb complex. To this end, 18 TNBC cell lines were treated with BRD4 inhibitor JQ1 for 96 hours at concentrations ranging from 0.0316-3.16 µM. An overwhelmingly refractory response to JQ1 was observed in the cell line panel (Figure 1A-B), except cell lines MDA-MB-231, MDA-MB-453 and SUM149PT, which were sensitive to JQ1 at doses lower than 1 µM. Next, to determine whether blocking P-TEFb function via CDK9 inhibition could sensitise TNBC cells to BRD4 inhibition by JQ1, the same panel of TNBC cell lines were treated with the same dose range of JQ1 combined with previously tested potent
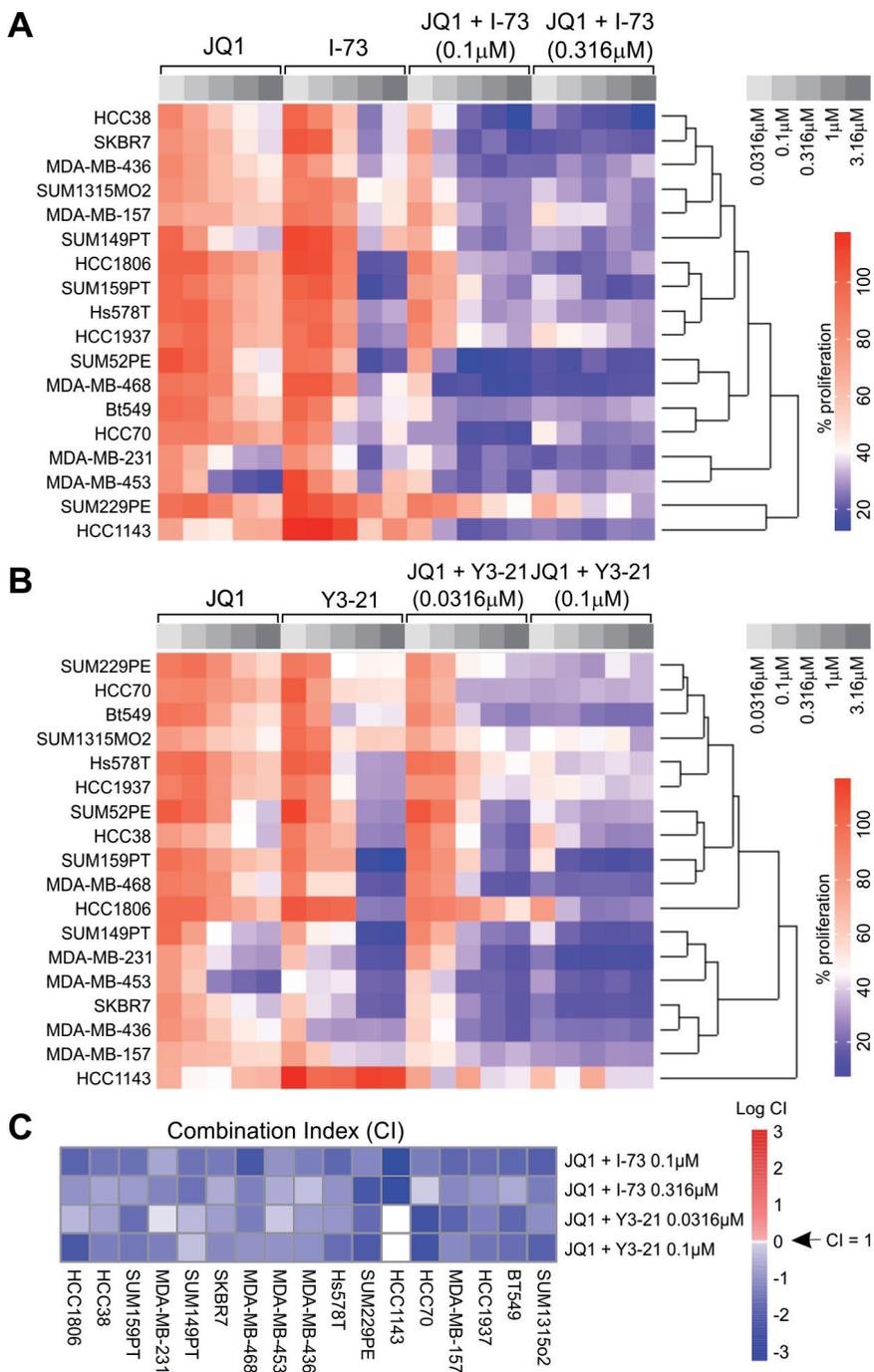
Figure 1. CDK9 inhibitors I-73 and Y3-21 synergise with BRD4 inhibitor JQ1 in TNBC cells. A. Anti-proliferative effect of combining JQ1 in a concentration range with I-73 (0.1 or 0.316μM) in a panel of TNBC cell lines. **B.** Anti-proliferative effect of combining JQ1 in concentration range with Y3-21 (0.0316 or 0.1μM) in a panel of TNBC cell lines. Proliferation was evaluated using SRB assay after 4 days' treatment. Results shown as percentage proliferation normalised to DMSO control. **C.** Combination index (CI) assessment of the synergistic effect of JQ1 + I-73 and JQ1 + Y3-21 on TNBC cell proliferation inhibition. The CI values were presented in natural logarithm (Log CI). CI > 1, antagonism; CI = 1, additivity; CI < 1, synergy.

CDK9 inhibitors I-73 (0.1µM or 0.316 µM) and Y3-21 (0.0316µM or 0.1 µM). These concentrations are ineffective or only slightly effective at inhibiting proliferation and P-TEFb signalling transduction in TNBC cells. Striking synergy was observed between JQ1 and I-73 (Figure 1A), as well as between JQ1 and Y3-21 (Figure 1B), as exemplified by synergistic combination indices (CI < 1.0) (Figure 1C), with superior reductions in cell proliferation compared to either I-73, Y3-21 or JQ1 alone. Furthermore, co-treatment with JQ1 (0.1 or 0.316 µM) and I-73 (0.1 µM) abolished P-TEFb-mediated phosphorylation of RNAPII at Ser2 and Ser5, respectively, in Hs578T, MDA-MB-157, HCC1143 and SUM149T cells (Figure 2A-D). RNAPII and the positive regulator BRD4 were also depleted as a result of the combination. Remarkably, CDK9 and BRD4 co-inhibition severely reduced levels of pro-survival BCL-2 family proteins MCL-1 and BCL-xL, and increased levels of γ-H2AX. These results indicate that simultaneously targeting CDK9 and BRD4 using I-73 and JQ1 is synergistic in TNBC cells, thereby eliminating P-TEFb/CDK9-mediated signal transduction and inducing DNA damage, consequently leading to cell death.

Targeting CDK9 overcomes resistance to EGFR inhibition in TNBC cells
TNBC cell lines highly express the receptor tyrosine kinase EGFR but are generally insensitive to EGFR-TKIs. Previously, we revealed that a dual cdc7/CDK9 inhibitor (PHA-767491) sensitises TNBC cells to EGFR-TKIs. Given the impact of combined P-TEFb and BET inhibition in TNBC, we further investigated whether I-73 would sensitise TNBC cells to EGFR-TKIs lapatinib or gefitinib. Co-treatment of a panel of EGFR-TKI-resistant TNBC cell lines with I-73 (0.1 µM or 0.316 µM) or Y3-21 (0.0316 µM or 0.1 µM) in combination with either lapatinib (0.0316-3.16 µM) or gefitinib (0.0316-3.16 µM) led to a remarkable reduction in cell proliferation 96 hours post-
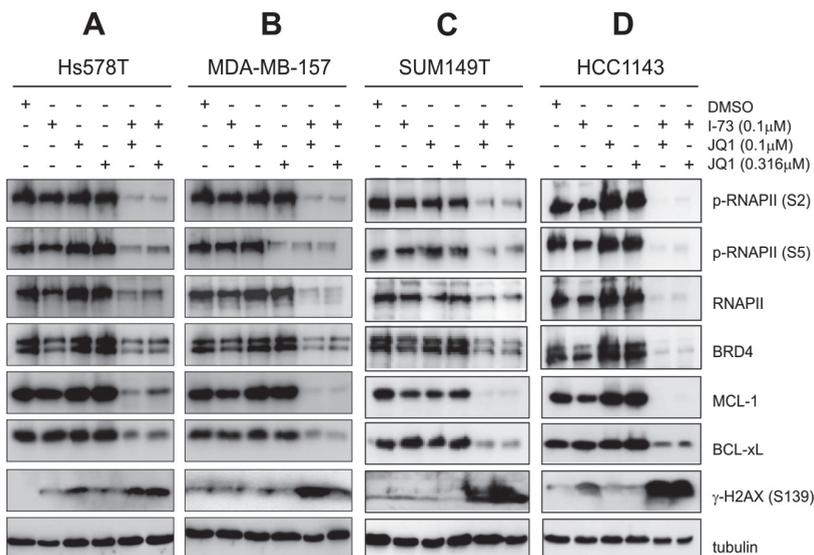
A Hs578T **B** MDA-MB-157 **C** SUM149T **D** HCC1143

+	-	-	-	-	-	DMSO
-	+	-	-	+	+	I-73 (0.1μM)
-	-	+	-	+	-	JQ1 (0.1μM)
-	-	-	+	-	+	JQ1 (0.316μM)

p-RNAPII (S2)
p-RNAPII (S5)
RNAPII
BRD4
MCL-1
BCL-xL
γ-H2AX (S139)
tubulin

Figure 2. Synergistic effect of I-73 and JQ1 on P-TEFb signalling and downstream targets. Immunoblot-based analysis showing the impact of JQ1 and I-73 co-treatment on inhibition of P-TEFb-mediated RNAPII Ser2/Ser5 phosphorylation, downregulation of the P-TEFb regulator BRD4, suppression of anti-apoptotic BCL-xL and MCL-1, and induction of apoptotic phospho-γ-H2AX in Hs578T (**A**), MDA-MB-157 (**B**), SUM149PT (**C**) and HCC1143 (**D**) TNBC cells. Cells were treated for 48 hours with I-73 (0.1μM), JQ1 (0.1 or 0.316μM) alone or combination as indicated. DMSO was used as control. Tubulin was used as sample loading control.

exposure, superior to either monotherapy (Figures 3A-B, Supplementary Figure S2). CI values well below 1.0 (CI < 1) indicated that the interaction between the EGFR-TKIs and the CDK9 inhibitors was synergistic in nature (Figure 3C). The synergistic effect of lapatinib and I-73 on proliferation inhibition was further validated in representative TNBC cell lines Hs578T, BT549 and SKBR7, further confirming the synergistic concentrations of I-73 (0.1-0.316 μM) (Figure 4A). Remarkably, co-treatment with I-73 (0.1 μM) and lapatinib induced apoptosis to a greater extent than lapatinib or I-73 alone in Hs578T, SUM149T, HCC1143, MDA-MB-436, MDA-MB-468 and MDA-MB-231 cells (Figure 4B). Immunoblot analysis revealed that apoptosis induction by co-treatment with lapatinib and I-73 was preceded by inhibition of RNAPII phosphorylation and subsequent depletion of MCL-1 (Figure 4C); I-73 at 0.1 μM only led to modest reduction in the levels of MCL-1 protein, but when combined
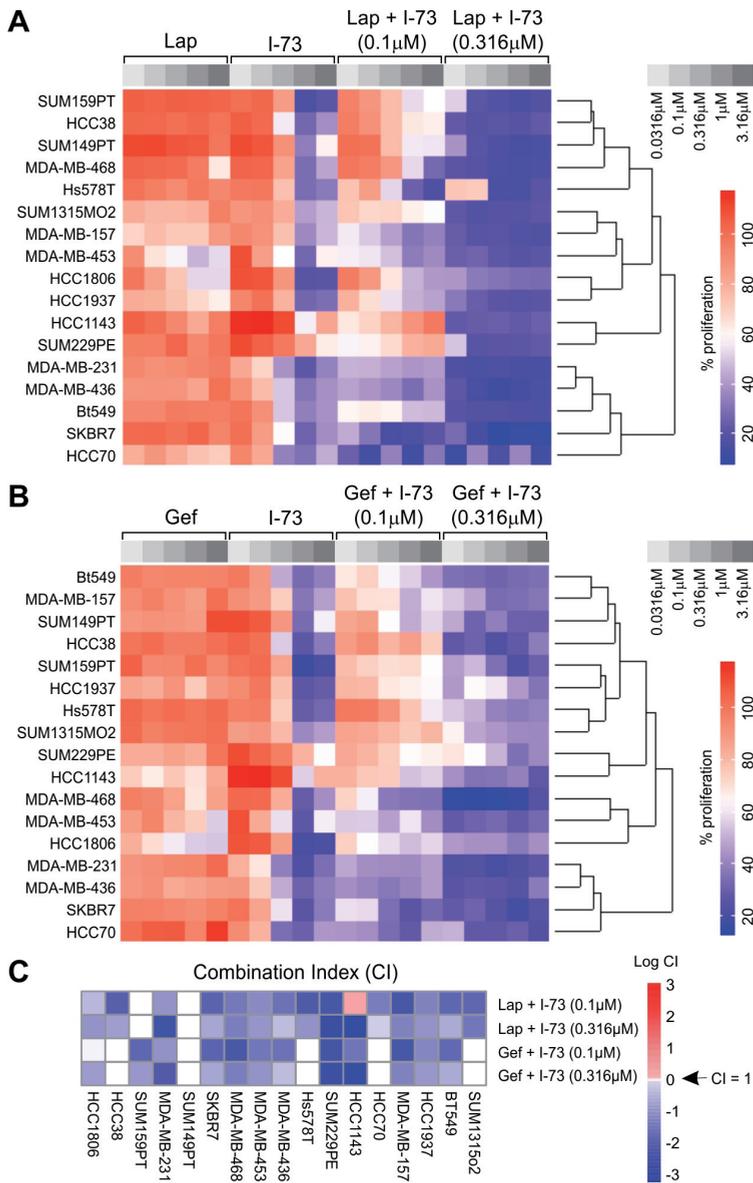
Figure 3. CDK9 inhibitor I-73 reverses the resistance of TNBC cells to EGFR-tyrosine kinase inhibitors. A. Effect of EGFR-TKI lapatinib (Lap) in concentration range combined with I-73 (0.1 μM or 0.316 μM) on the proliferation of TNBC cell lines. **B.** Effect of EGFR-TKI gefitinib (Gef) in concentration range combined with I-73 (0.1 μM or 0.316 μM) on the proliferation of TNBC cell lines. Data shown as percentage proliferation normalised to DMSO control. **C.** Synergistic CI evaluation of Lap + I-73 and Gef + I-73 combinations. Data shown as Log CI values. CI > 1, antagonism; CI = 1, additivity; CI < 1, synergy.
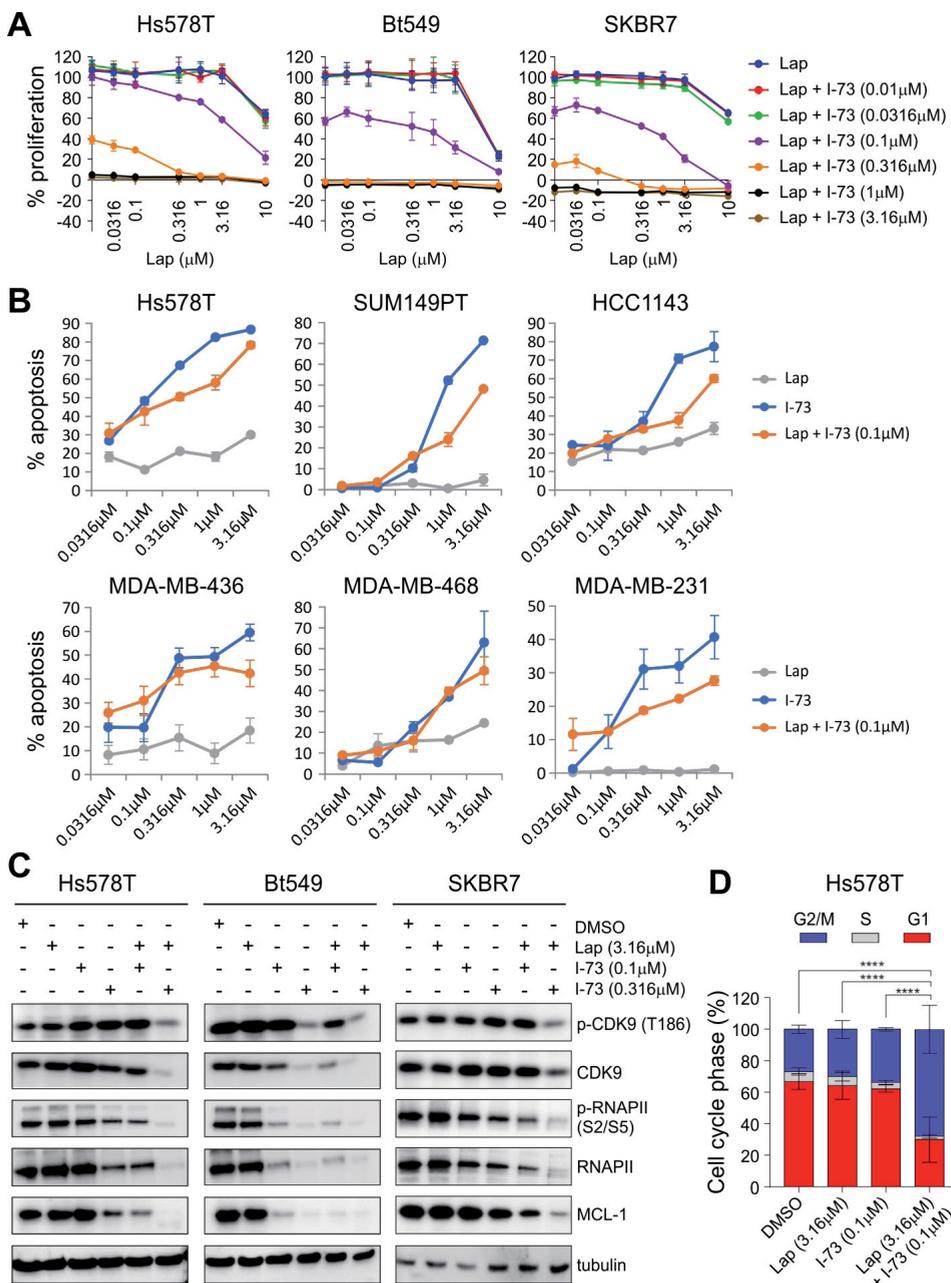
Figure 4. Synergistic effect of I-73 and lapatinib on P-TEFb signalling inhibition, cell cycle G2/M arrest and apoptosis induction. A. Dose response matrix combination of I-73 and lapatinib (Lap) in TNBC cell lines Hs578T, BT549 and SKBR7, Data shown as percentage proliferation normalised to DMSO control. Representative of three independent experiments performed in triplicate. **B.** I-73 and lapatinib combination induced apoptosis in TNBC cell lines Hs578T, SUM149T, HCC1143, MDA-MB-436, MDA-MB-468 and MDA-MB-231. Cells were treated with lapatinib, I-73, or a concentration range of lapatinib combined with I-73 at 0.1 μM for 72 hours. Induction of apoptosis was measured by calculating the percentage Annexin V-positive cells normalised to Hoechst-positive cells. Data shown as mean +/- standard deviation (n = 2). **C.** I-73 and lapatinib synergistic effect on inhibition of P-TEFb-mediated RNAPII phosphorylation and down-regulation of anti-apoptotic protein MCL-1 in Hs578T, BT549 and SKBR7 TNBC cells. Cells were harvested after 48 hours' co-treatment with I-73 and lapatinib, as indicated. **D.** I-73 and lapatinib co-treatment induced superior G2/M cell cycle arrest in Hs578T cells, compared to either monotherapy. Data were shown as percentage cells per cell cycle phase (G2/M, S or G1) normalized to DMSO control, and represented as mean +/- standard deviation (n = 4). Two-way ANOVA with Tukey's multiple comparison test; ****p < 0.0001.

with lapatinib MCL-1 was completely ablated in Hs578T and BT549 cells 48 hours post-treatment. I-73 at 0.316 µM drastically depleted MCL-1 levels in Hs578T, BT549 and SKBR7 cells, this effect also being enhanced upon addition of lapatinib at 3.16 µM. Consistent with the induction of apoptosis, the combination of lapatinib and I-73 induced strong G2/M cell cycle arrest to a significantly greater extent than single treatment with either lapatinib (3.16 µM) or I-73 (0.1 µM) (Figure 4D). In short, the resistance of TNBC cells to EGFR-TKIs can be reversed by combining such agents with CDK9 inhibitors, leading to apoptosis and cell cycle arrest.

Co-inhibition of EGFR and CDK9 profoundly alters gene transcription in TNBC cells

To illuminate the transcriptional changes associated with the CDK9 inhibition-mediated reversal of intrinsic resistance to EGFR-TKIs in TNBC cells, we performed RNA sequencing-based transcriptomic analysis of Hs578T TNBC cells treated for 6 hours with lapatinib (3.16 µM), I-73 (0.1 µM) and their combination, respectively. By normalizing treatment conditions to control conditions, a cut-off of Log2 fold change (Log2 FC) ≥ ±0.68 (FC = 1.5) was used to classify significantly differentially expressed genes after treatment with monotherapies (I-73 at 0.1 µM or lapatinib at 3.16 µM) or combination. Comparing the transcripts which were differentially expressed under co-treatment with those altered under single treatment with either lapatinib (Lap + I-73 vs Lap, Log2 FC ≥ ±0.68) or I-73 (Lap + I-73 vs I-73, Log2 FC ≥ ±0.68), identified a total of 2220 overlapping genes, 529 of which were up-regulated and 1691 of which were down-regulated (Figure 5A). These 2220 genes were selected as lapatinib and I-73 synergy-related genes. Ingenuity Pathway Analysis (IPA)-based assessment of the synergy-related transcripts revealed an enrichment of genes involved in mammalian embryonic stem cell pluripotency, TGF-β

signalling, regulation of cell cycle progression, and JAK-STAT canonical signalling pathways, amongst others, in the down-regulated set (Figure 5B). This set of genes was mainly clustered in regulatory networks of gene transcription and expression as well as protein ubiquitination (Figure 5C). Clearly, I-73 strongly synergised with lapatinib to target genes which were insensitive to EGFR inhibition alone, particularly those involved in stem cell pluripotency (Figure 5D), G1/S checkpoint regulation (Figure 5E), and TGF-β signalling (Figure 5F). For instance, the expression of SMAD1, BMP4, TRAF6, ACVR2A and PITX2, which are crucial for Wnt/β-catenin-, TGF-β- and BMP-mediated signal transduction as well as activation of downstream JNK and p38-MAPK kinases[42,43], was inhibited by I-73 and this effect was augmented after combination with lapatinib (Figure 5F). Additionally, the I-73-mediated inhibition of key regulators of mammalian embryonic stem cell pluripotency associated with EMT (e.g. RARA)[44] and a chemo-resistant cancer stem cell phenotype (KDM5B)[45], was also enhanced by the addition of lapatinib (Figure 5D). Similarly, co-treatment of Hs578T cells with I-73 and lapatinib potentiated the inhibitory effect of I-73 on 293 transcription regulatory genes (Figure 6A). These included ZNF, FOX, E2F and KLF transcription factor family members (Figure 6B). Strikingly, the synergistic interaction of lapatinib and I-73 potently blocked P-TEFb transcriptional function by targeting genes involved in transcription initiation (Figure 6C), including E2F2, E2F3, and CDK9 itself, as well as targets downstream of BRD4 (Figure 6D), such as BCL1L1, MCL1, CDC25[46]. Thus, lapatinib potentiates the inhibitory effects of I-73 on transcriptional regulators, thereby shutting down pathways critical for cancer cell survival and adaptation to targeted agents. Furthermore, while lapatinib synergized with I-73 in gene expression regulation, their

synergistic effect also resulted in suppression of multiple growth factor-mediated networks, such as IGF, HGF, MBP and GDF, which guide alternative RTK-mediated signal transduction (Supplementary Figure S3A), Of relevance, MEK signalling downstream of RTKs was strongly attenuated (Supplementary Figure S3B), a number of genes being vulnerable to the synergistic effect, including SPRY2, RND3, and pro-survival BCL-2 members BCL2L1, BCL1L11 and MCL1. In particular, these results are therefore relevant to circumstances where TNBC cells are addicted to oncogenic growth factor- and RTK-mediated signalling and where TNBC cells are resistant to MEK inhibition.

Transcriptional regulators sensitive to CDK9 and EGFR co-inhibition are associated with poor prognosis in TNBC patients

Considering the profound inhibition of expression of transcriptional regulators after co-treatment with I-73 and lapatinib, we subsequently evaluated the association between expression of these transcripts and metastasis-free survival (MFS) in a cohort of 142 TNBC patients. Amongst 293 synergy-related transcriptional regulators, high expression of 15 transcription factors, which were strongly down-regulated by co-treatment with lapatinib and I-73, was associated with a significantly poorer MFS in this cohort (Figure 7A). These included TRIM13, KLF9, DACT1, KLF2, GTF2E1, KLF6, PITX2, JMID1C, GATA2, RBM5, FOXO1, ZFP36, RRPB, PPM1D and NOS1AP. Multiple Kruppel-like family (KLF) transcription factors were down-regulated by co-treatment (Figure 6B), with high expression levels of KLF2, KLF6 and KLF9 being significantly correlated with a poor MFS in TNBC patients (Figure 7A). Representative Kaplan-Meier (KM) survival curves for TRIM13, DACT1, KLF9, and KLF6 are shown (Figure 7B). These data suggest that CDK9 and EGFR co-targeted
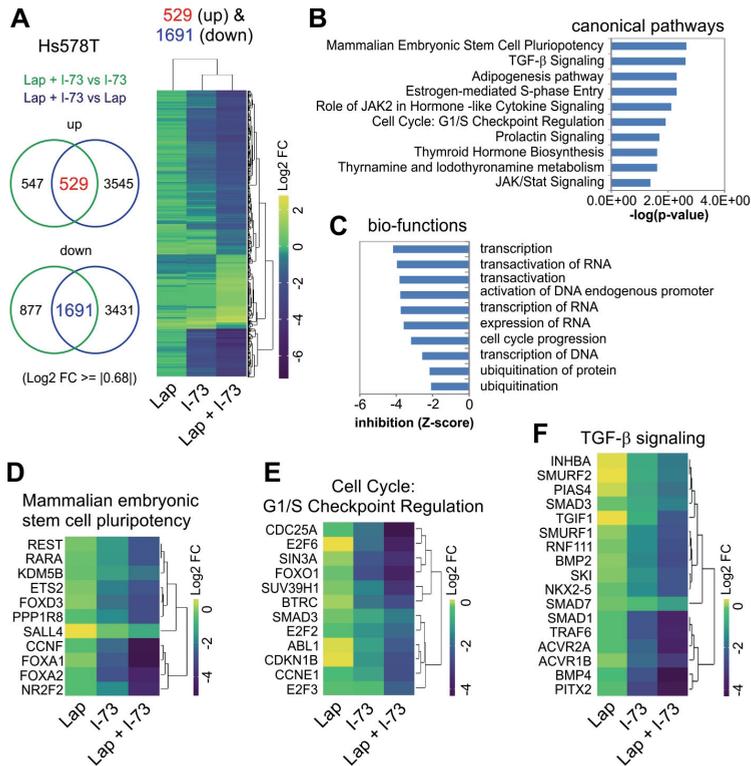
Figure 5. I-73 and lapatinib co-treatment disrupts the transcriptomic profile of TNBC cells. TNBC Hs578T cells were treated for 6 hours with Lap (3.16μM), I-73 (0.1μM), combined Lap + I-73 at the same doses, or DMSO as control, and harvested for RNA purification and RNA-Sequencing, Gene expression levels were presented in Log2 fold change (Log2 FC) normalized to control DMSO. **A.** Venn diagram and clustering of 529 up- and 1691 down-regulated genes in I-73 and lapatinib combination. Expression levels of genes under Lap + I-73 combined treatment were compared to those under single treatment Lap (Lap + I-73 vs Lap) or I-73 (Lap + I-73 vs I-73), Genes that overlapped in both comparisons and which were significantly up- (Log2 FC ≥ +0.68) or down-regulated (Log2 FC ≤ -0.68), were selected as synergy-related genes. The differential expression signature is shown in the heatmap. **B**. Top canonical pathways in which the Lap + I-73 synergy-regulated and differentially expressed genes are enriched, revealed by Ingenuity Pathway Analysis® (IPA). Significance was presented as –log p(value). **C.** Enrichment of Lap + I-73 synergy-related genes in top biological functions. Inhibitory effect was presented as Z-score. **D.** Expression of Lap + I-73 synergy-sensitive factors regulating mammalian embryonic stem cell pluripotency. **E.** Regulators of G1/S cell cycle in response to Lap + I-73 synergy. **F.** Sensitivity of TGF-β pathway members to Lap + I-73 synergy.

therapies are potentially effective in down-regulating transcription factors that are expressed at higher levels in TNBC tumours and which are correlated with poor disease outcomes in TNBC patients.
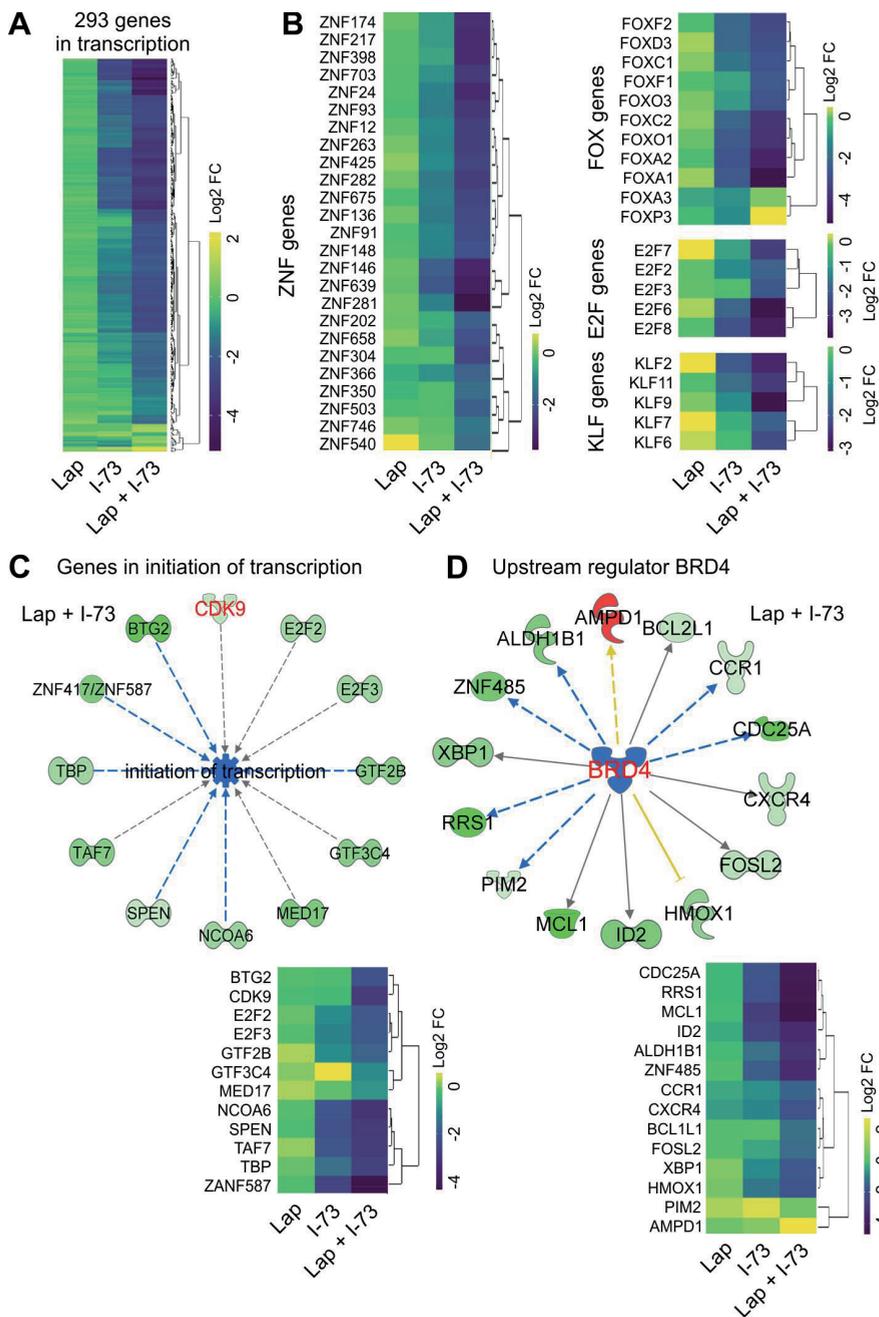
Figure 6. Synergistic effect of I-73 and lapatinib on P-TEFb-mediated transcription regulators. A. 293 Lap + I-73 synergy-related genes functioning as transcription regulators. **B.** Sensitivity of ZNF, FOX, E2F and KLF transcription factor family members to Lap + I-73 synergy. **C.** Disruption of CDK9 involved transcription initiation by Lap + I-73 synergy. **D.** Suppression of BRD4 downstream targets by Lap + I-73 synergy. The colours of the nodes are as follows; red represents up-regulation, green represents down-regulation, and blue indicates inhibition. The colours of the lines indicating effects are as follows: blue represents inhibition, yellow indicates an inconsistent effect, whereas grey represents events lacking prediction.

A

Symbol	HR	pval	95% CI low	95% CI high	Lap Log2 FC	I-73 Log2 FC	Lap + I-73 Log2 FC
TRIM13	3.00	0.001	1.58	5.71	-0.32	-1.55	-3.03
KLF9	2.53	0.002	1.39	4.61	0.02	-1.04	-3.03
DACT1	1.71	0.003	1.20	2.44	0.12	-2.86	-3.89
KLF2	1.79	0.003	1.22	2.65	0.16	-1.94	-2.68
GTF2E1	2.43	0.012	1.22	4.83	-0.01	-1.66	-3.90
PITX2	3.75	0.013	1.32	10.63	-0.17	-2.77	-4.09
KLF6	1.79	0.014	1.13	2.86	0.10	-0.22	-2.20
JMJD1C	1.70	0.024	1.07	2.69	0.10	-1.25	-2.56
GATA2	1.92	0.025	1.09	3.40	-0.21	-1.26	-3.25
RBM5	2.03	0.027	1.08	3.81	-0.01	-1.41	-3.49
FOXO1	1.59	0.033	1.04	2.45	-0.13	-2.54	-3.86
ZFP36	1.74	0.036	1.04	2.91	0.32	-1.36	-2.51
RRP8	2.49	0.038	1.05	5.91	-0.17	-0.30	-2.58
PPM1D	1.95	0.038	1.04	3.68	-0.08	-1.35	-2.77
NOS1AP	3.71	0.040	1.06	12.96	-0.09	-0.47	-1.34

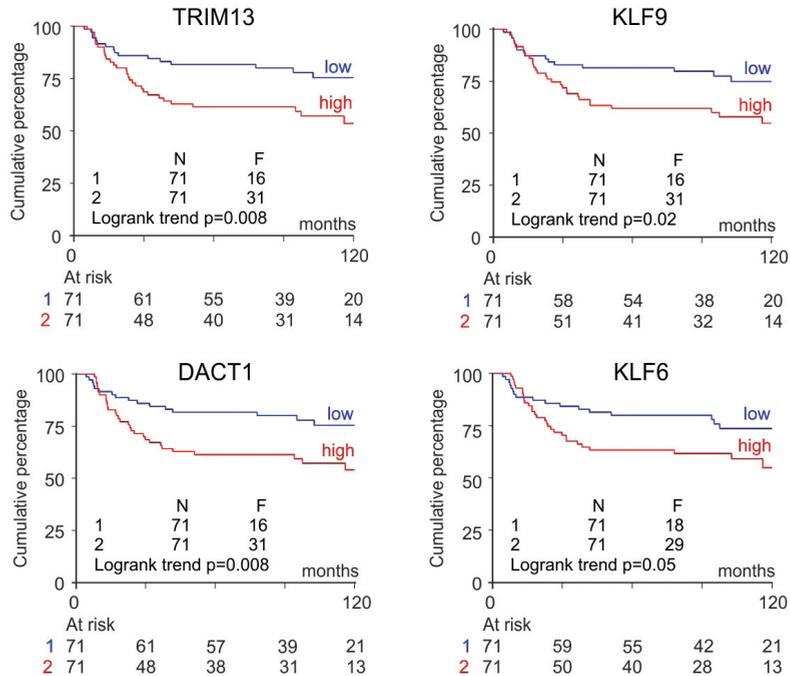Header note: TNBC patients | RNA-seq TNBC Hs578T cells

B

Figure 7. Clinical relevance of transcription factors down-regulated by I-73 and lapatinib co-treatment in TNBC patients. **A.** Fifteen Lap + I-73 synergy-related transcription factors in association with TNBC clinical outcome. Evaluation was based on the cohort of 142 TNBC patients (Erasmus Medical Rotterdam data and public data), Metastasis-free survival (MFS) was taken as end point. Hazard ratio (HR), p-value (pval) and 95% confidence intervals (95% CI) were based on Cox univariate regression analysis. Lap Log2 FC, I-73 Log2 FC and combined Lap + I-73 Log2 FC, show inhibitory effect on gene expression, as revealed by RNA-Seq transcriptomic analysis in TNBC Hs578T cells. **B.** Representative Kaplan-Meier (KM) MFS survival curves for 142 TNBC patients with expression of Lap + I-73 synergy-related genes TRIM13, DACT1, KLF9 or KLF6.

DISCUSSION

TNBC is an aggressive, heterogeneous, difficult-to-treat subtype of breast cancer which at present cannot be successfully treated with effective targeted agents designed to exploit the specific dependencies of these tumours[32,47]. EGFR-targeted therapy in the form of anti-EGFR monoclonal antibodies or EGFR-TKIs has yet to show tangible clinical benefit in TNBC patients, despite high levels of EGFR expression in TNBC tumours, highlighting the need for rational combination therapies[23,48]. One of the major obstacles to the development of such molecular targeted therapies is the presence of *de novo* resistance or the subsequent development of acquired resistance[21,49]. In order to address these issues, we utilised CDK inhibitors I-73 and Y3-21 with potent activity against P-TEFb/CDK9 to sensitise drug-resistant TNBC to EGFR-TKIs, thereby demonstrating that co-inhibition of EGFR and CDK9 represents a valid strategy to sensitise TNBC cells to EGFR-TKIs currently in clinical practice.

Here, we show that I-73 and Y3-21 were capable of abrogating the refractory response of TNBC cells to JQ1, with down-regulation of MCL-1 only observed after co-treatment. Combined inhibition of BRD4 and CDK9 has recently been assessed in an *in vitro* model of rhabdoid tumours, in which co-treatment with JQ1 and LDC000067 down-regulated the expression of anti-apoptotic genes and known oncogene c-MYC leading to apoptosis induction *in vitro* and profound reductions in tumour growth *in vivo*[50]. CDK9 inhibition is also synthetic lethal with presence of the BRD4-NUT fusion oncogene in NUT midline carcinoma (NMT), where CDK9 represents as a non-oncogenic addiction due to its critical role in regulating transcriptional elongation and MYC expression[51]. Similar to the results described

herein, CDK9 inhibition led to depletion of MCL-1, enhanced γ-H2AX and induction of cell death[51]. All these data support the assertion that CDK9 and BRD4, the major controllers of P-TEFb transcriptional function, are potential targets in cancers addicted to aberrant transcription. Further validation of this synergy between CDK9 and BRD4 inhibition requires a more extensive array of BET inhibitors. In this regard, using BET inhibitors currently under investigation in clinical trials for TNBC or other solid malignancies, such as I-BET762, OTX015 or BAY1238097, would be of relevance[52].

To our knowledge, this study is the first to demonstrate that the CDK9 inhibitors I-73 and Y3-21 sensitise TNBC cells to EGFR-TKIs lapatinib and gefitinib, and to investigate the transcriptional disruption associated with co-treatment. Co-treatment of EGFR-TKI-resistant TNBC cells with lapatinib and I-73 potently inhibits TNBC cell proliferation, induces apoptosis associated with profound G2/M cell cycle arrest, in a manner superior to either monotherapy. Transcriptomic profiling revealed that synergistic inhibition of EGFR and CDK9 led to transcriptional reprogramming in EGFR-TKI-resistant TNBC cells. Co-treatment down-regulated CDK9 and components involved in transcription initiation, thereby suppressing expression of transcription factors such as ZNF, FOX, E2F and KLF, as well as those involved in regulating stem cell pluripotency, G1/S checkpoint and TGF-β signalling. Crucially, this transcriptional reprogramming suppresses numerous downstream targets of IGF, HGF, GDF and MBP growth factor-mediated networks, including the MEK signalling pathway. This could highlight a promising strategy for overcoming adaptive resistance to other RTK- and MEK-targeted therapies, in TNBC and also other cancer types.

A selection of the lapatinib and I-73 synergy-related transcription factors found to be highly expressed in a subset of TNBC tumours were linked to a significantly poorer MFS in TNBC and breast cancer patients in general. Most strikingly, a group of KLF transcription factors, including KLF2, KLF6 and KLF9, were associated with poor clinical outcome. Additionally, our previous work confirmed that a number of these factors, including GATA2, are indispensable factors for TNBC cell proliferation *in vitro*. DACT1 prevents the degradation of β-catenin associated with enhanced GSK-3β phosphorylation, thereby promoting its nuclear translocation and the subsequent transcriptional activation of genes downstream of Wnt/β-catenin-mediated signal transduction[53]. Chromatin immunoprecipitation in ovarian carcinoma cell lines demonstrated that PITX2 is frequently associated with gene promoters downstream of Wnt/β-catenin signalling, and that PITX2 itself can directly activate canonical Wnt signalling[54]. Further functional evaluation of the role of these transcription factors in the control of TNBC proliferation and EGFR-related signal transduction is therefore warranted.

In conclusion, we provide evidence that CDK inhibitors potently targeting CDK9 activity sensitise TNBC cells to the BET inhibitor JQ1 and the EGFR-TKIs lapatinib and erlotinib. Co-treatment of TNBC cell lines with lapatinib and I-73 induces apoptosis and cell cycle arrest associated with depletion of pro-survival factors, profound inhibition of transcription, and obstruction of growth factor-mediated downstream MAPK signalling networks, as evidenced by transcriptomic profiling. This co-treatment preferentially inhibits the function of multiple transcription factors, some of which are significantly associated with poor prognosis in TNBC patients.

Further evaluation of the synergistic interactions in an *in vivo* context, as well as functional genomic studies of synergy-sensitive transcription factors, would be beneficial for ascertaining the true clinical relevance of such combination therapies.

FUNDING

REFERENCES

1. Boyle, P. Triple-negative breast cancer: epidemiological considerations and recommendations. *Ann. Oncol.* **23 Suppl 6,** vi7-12 (2012).

2. de Ruijter, T. C., Veeck, J., de Hoon, J. P. J., van Engeland, M. & Tjan-Heijnen, V. C. Characteristics of triple-negative breast cancer. *J. Cancer Res. Clin. Oncol.* **137,** 183–92 (2011).

3. Dent, R. *et al.* Pattern of metastatic spread in triple-negative breast cancer. *Breast Cancer Res. Treat.* **115,** 423–8 (2009).

4. Kalimutho, M. *et al.* Targeted Therapies for Triple-Negative Breast Cancer: Combating a Stubborn Disease. *Trends Pharmacol. Sci.* **36,** 822–46 (2015).

5. Masuda, H. *et al.* Differential response to neoadjuvant chemotherapy among 7 triple-negative breast cancer molecular subtypes. *Clin. Cancer Res.* **19,** 5533–40 (2013).

6. Radovich, M. *et al.* Characterizing the heterogeneity of triple-negative breast cancers using microdissected normal ductal epithelium and RNA-sequencing. *Breast Cancer Res. Treat.* **143,** 57–68 (2014).

7. Irshad, S., Ellis, P. & Tutt, A. Molecular heterogeneity of triple-negative breast cancer and its clinical implications. *Curr. Opin. Oncol.* **23,** 566–577 (2011).

8. Hnisz, D. *et al.* Convergence of Developmental and Oncogenic Signaling Pathways at Transcriptional Super-Enhancers. *Mol. Cell* **58,** 362–370 (2015).

9. Zawistowski, J. S. *et al.* Enhancer remodeling during adaptive bypass to MEK inhibition is attenuated by pharmacologic targeting of the P-TEFb complex. *Cancer Discov.* **7,** 302–321 (2017).

10. Ahn, S. H., Kim, M. & Buratowski, S. Phosphorylation of serine 2 within the RNA polymerase II C-terminal domain couples transcription and 3' end

processing. *Mol Cell* **13,** 67–76 (2004).

11. Moon, K. J. *et al.* The bromodomain protein Brd4 is a positive regulatory component of P-TEFb and stimulates RNA polymerase II-dependent transcription. *Mol. Cell* **19,** 523–534 (2005).

12. Peterlin, B. M. & Price, D. H. Controlling the Elongation Phase of Transcription with P-TEFb. *Molecular Cell* **23,** 297–305 (2006).

13. Itzen, F., Greifenberg, A. K., Christian, A. B. & Geyer, M. Brd4 activates P-TEFb for RNA polymerase II CTD phosphorylation. **42,** 7577–7590 (2014).

14. Yang, Z. *et al.* Recruitment of P-TEFb for stimulation of transcriptional elongation by the bromodomain protein Brd4. *Mol. Cell* **19,** 535–545 (2005).

15. Lam, F. *et al.* Targeting RNA transcription and translation in ovarian cancer cells with pharmacological inhibitor CDKI-73. *Oncotarget* **5,** 7691–704 (2014).

16. Gao, Y., Liang, Y., Zhang, T., Gray, N. S. & George, R. E. Optimizing selective CDK7 inhibition in MYCN-driven neuroblastoma. *Mol. Cancer Ther.* **14,** (2015).

17. Cayrol, F. *et al.* THZ1 targeting CDK7 suppresses STAT transcriptional activity and sensitizes T-cell lymphomas to BCL2 inhibitors. *Nat. Commun.* **8,** 14290 (2017).

18. Xie, S. *et al.* Antitumor action of CDK inhibitor LS-007 as a single agent and in combination with ABT-199 against human acute leukemia cells. *Acta Pharmacol. Sin.* **37,** 1–9 (2016).

19. Wang, Y. *et al.* CDK7-Dependent Transcriptional Addiction in Triple-Negative Breast Cancer. *Cell* **163,** 174–186 (2015).

20. Duncan, J. S. *et al.* Dynamic reprogramming of the kinome in response to targeted MEK inhibition in triple-negative breast cancer. *Cell* **149,** 307–21 (2012).

21. Groenendijk, F. H. & Bernards, R. Drug resistance to targeted therapies: déjà vu all over again. *Mol. Oncol.* **8,** 1067–83 (2014).

22. Stuhlmiller, T. J. *et al.* Inhibition of lapatinib-induced kinome reprogramming in ERBB2-positive breast cancer by targeting BET family bromodomains. *Cell Rep.* **11,** 390–404 (2015).

23. Nakai, K., Hung, M. C. & Yamaguchi, H. A perspective on anti-EGFR therapies targeting triple-negative breast cancer. *American Journal of Cancer Research* **6,** 1609–1623 (2016).

24. Secq, V. *et al.* Triple negative breast carcinoma EGFR amplification is not associated with EGFR, Kras or ALK mutations. *Br. J. Cancer* **110,** 1045–52 (2014).

25. Martin, V. *et al.* Molecular characterization of EGFR and EGFR-downstream pathways in triple negative breast carcinomas with basal like features. *Histol. Histopathol.* **27,** 785–792 (2012).

26. Baselga, J. *et al.* Randomized phase II study of the anti-epidermal growth factor receptor monoclonal antibody cetuximab with cisplatin versus cisplatin alone in patients with metastatic triple-negative breast cancer. *J. Clin. Oncol.* **31,** 2586–92 (2013).

27. Dickler, M. N., Cobleigh, M. a, Miller, K. D., Klein, P. M. & Winer, E. P. Efficacy and safety of erlotinib in patients with locally advanced or metastatic breast cancer. *Breast Cancer Res. Treat.* **115,** 115–21 (2009).

28. Schuler, M. *et al.* A phase II trial to assess efficacy and safety of afatinib in extensively pretreated patients with HER2-negative metastatic breast cancer. *Breast Cancer Res. Treat.* **134,** 1149–1159 (2012).

29. Fujita, T., Ryser, S., Piuz, I. & Schlegel, W. Up-Regulation of P-TEFb by the MEK1-Extracellular Signal-Regulated Kinase Signaling Pathway Contributes to Stimulated Transcription Elongation of Immediate Early Genes in Neuroendocrine Cells. *Mol. Cell. Biol.* **28,** 1630–1643 (2008).

30. Bonnet, F., Vigneron, M., Bensaude, O. & Dubois, M. F. Transcription-independent phosphorylation of the RNA polymerase II C-terminal domain (CTD) involves ERK kinases (MEK1/2). *Nucleic Acids Res.* **27,** 4399–4404 (1999).

31. Baselga, J. *et al.* Phase II and tumor pharmacodynamic study of gefitinib in patients with advanced breast cancer. *J. Clin. Oncol.* **23,** 5323–33 (2005).

32. Lehmann, B. D. *et al.* Refinement of Triple-Negative Breast Cancer Molecular Subtypes: Implications for Neoadjuvant Chemotherapy Selection. *PLoS One* **11,** e0157368 (2016).

33. Walsby, E. *et al.* A novel Cdk9 inhibitor preferentially targets tumor cells and synergizes with fludarabine. *Oncotarget* **5,** 375–85 (2014).

34. Vichai, V. & Kirtikara, K. Sulforhodamine B colorimetric assay for cytotoxicity screening. *Nat. Protoc.* **1,** 1112–1116 (2006).

35. Zhang, Y. *et al.* Elevated insulin-like growth factor 1 receptor signaling induces antiestrogen resistance through the MAPK/ERK and PI3K/Akt signaling routes. *Breast Cancer Res.* **13 (3):** R52 (2011).

36. Robinson, M. D., McCarthy, D. J. & Smyth, G. K. edgeR: a Bioconductor package for differential expression analysis of digital gene expression data. *Bioinformatics* **26,** 139–40 (2010).

37. McCall, M. N., Bolstad, B. M. & Irizarry, R. A. Frozen robust multiarray analysis

(fRMA). *Biostatistics* **11,** 242–253 (2010).

38. Johnson, W. E., Li, C. & Rabinovic, A. Adjusting batch effects in microarray expression data using empirical Bayes methods. *Biostatistics* **8,** 118–127 (2007).

39. Huang, L., Jiang, Y. & Chen, Y. Predicting Drug Combination Index and Simulating the Network-Regulation Dynamics by Mathematical Modeling of Drug-Targeted EGFR-ERK Signaling Pathway. *Sci. Rep.* **7:** 40752 (2017).

40. Chou, T. C. Drug combination studies and their synergy quantification using the chou-talalay method. *Cancer Research* **70,** 440–446 (2010).

41. Foucquier, J. & Guedj, M. Analysis of drug combinations: current methodological landscape. *Pharmacology Research and Perspectives* **3 (3):** e00149 (2015).

42. Yu, L., Hébert, M. C. & Zhang, Y. E. TGF-β receptor-activated p38 MAP kinase mediates Smad-independent TGF-beta responses. *EMBO J.* **21,** 3749–59 (2002).

43. Mori, S. *et al.* TGF-β and HGF transmit the signals through JNK-dependent Smad2/3 phosphorylation at the linker regions. *Oncogene* **23,** 7416–7429 (2004).

44. Doi, A. *et al.* Enhanced expression of retinoic acid receptor alpha (RARA) induces epithelial-to-mesenchymal transition and disruption of mammary acinar structures. *Mol. Oncol.* **9,** 355–364 (2015).

45. Kuo, Y.-T. *et al.* JARID1B Expression Plays a Critical Role in Chemoresistance and Stem Cell-Like Phenotype of Neuroblastoma Cells. *PLoS One* **10 (5):** e0125343 (2015).

46. Hong, S. H. *et al.* Epigenetic reader BRD4 inhibition as a therapeutic strategy to suppress E2F2-cell cycle regulation circuit in liver cancer. *Oncotarget* **7(22):** 32628-40 (2016).

47. Bayraktar, S. & Glück, S. Molecularly targeted therapies for metastatic triple-negative breast cancer. *Breast Cancer Research and Treatment* **138,** 21–35 (2013).

48. Bernsdorf, M. *et al.* Effect of adding gefitinib to neoadjuvant chemotherapy in estrogen receptor negative early breast cancer in a randomized phase II trial. *Breast Cancer Res. Treat.* **126,** 463–470 (2011).

49. Pazarentzos, E. & Bivona, T. G. Adaptive stress signaling in targeted cancer therapy resistance. *Oncogene* **34,** 5599–606 (2015).

50. Moreno, N. *et al.* Combined BRD4 and CDK9 inhibition as a new therapeutic

approach in malignant rhabdoid tumors. *Oncotarget* **8(49):** 84986-84995 (2017).

51. Brägelmann, J. *et al.* Systematic Kinase Inhibitor Profiling Identifies CDK9 as a Synthetic Lethal Target in NUT Midline Carcinoma. *Cell Rep.* **20,** 2833–2845 (2017).

52. Erez-Salvia, M. P. & Esteller, M. Bromodomain inhibitors and cancer therapy: From structures to applications. *Epigenetics* **12 (5):** 323-339 (2017).

53. Yuan, G. *et al.* Oncogenic function of DACT1 in colon cancer through the regulation of β-catenin. *PLoS One* **7 (3):** e34004 (2012).

54. Basu, M. & Roy, S. S. Wnt/jS-catenin pathway is regulated by PITX2 homeodomain protein and thus contributes to the proliferation of human ovarian adenocarcinoma cell, SKOV-3. *J. Biol. Chem.* **288,** 4355–4367 (2013).
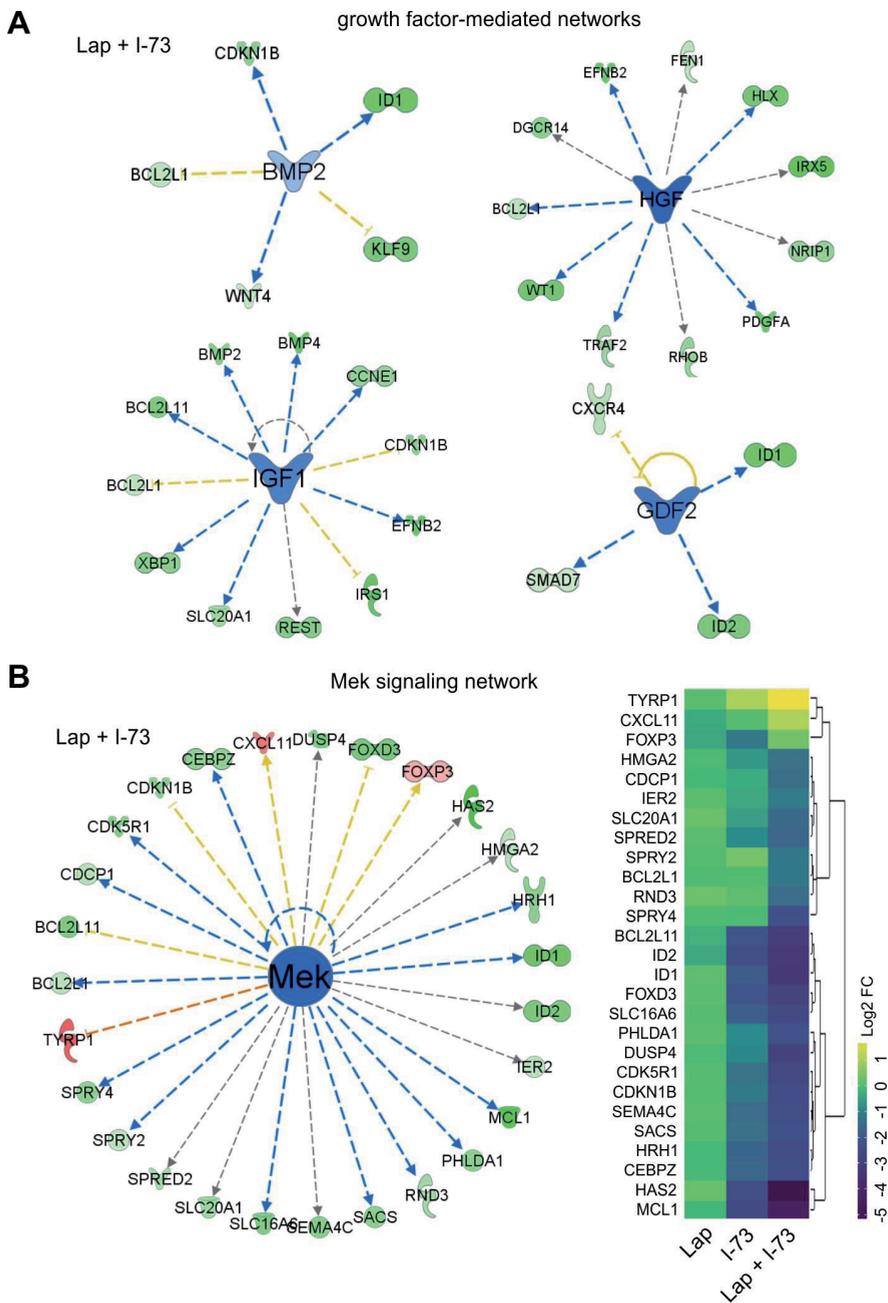
SUPPLEMENTARY FIGURES (OVERLEAF)
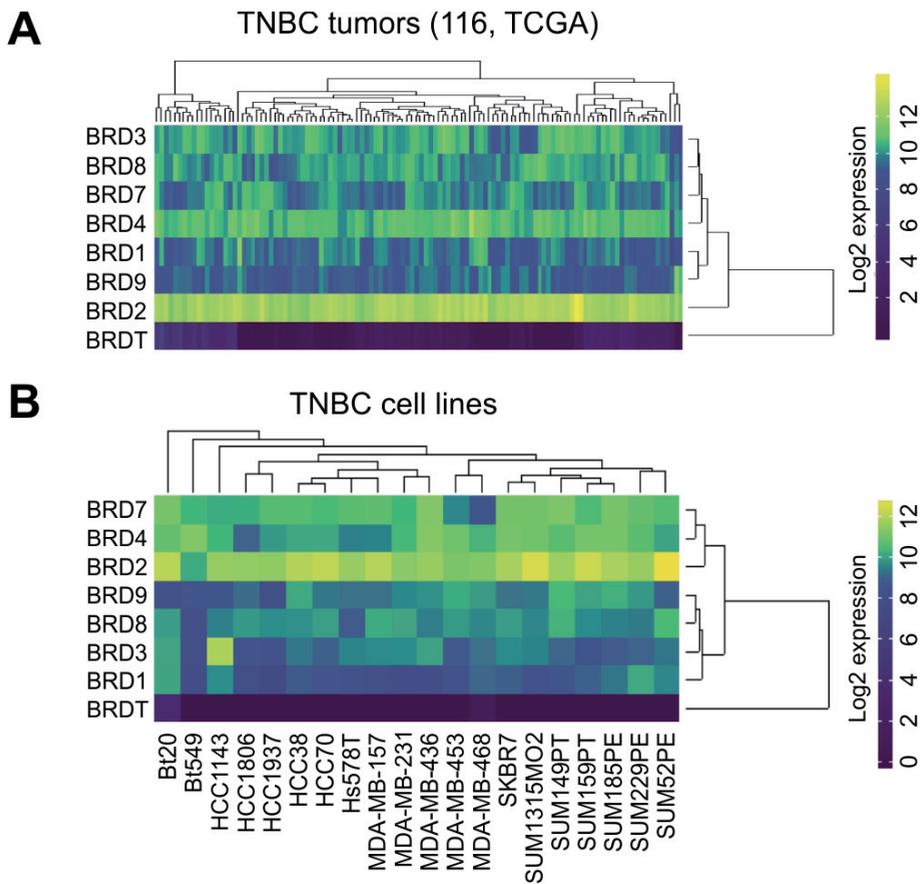
Supplementary Figure S1. A. Expression of BRD family members in 116 patient TNBC tumours. Data derived from TCGA RNA-Seq database. Data shown as RNA-seq-based Log$_2$ expression level. **B.** Expression of BRD family members in a panel of TNBC cell lines. Data shown as RNA-seq-based Log$_2$ expression level.
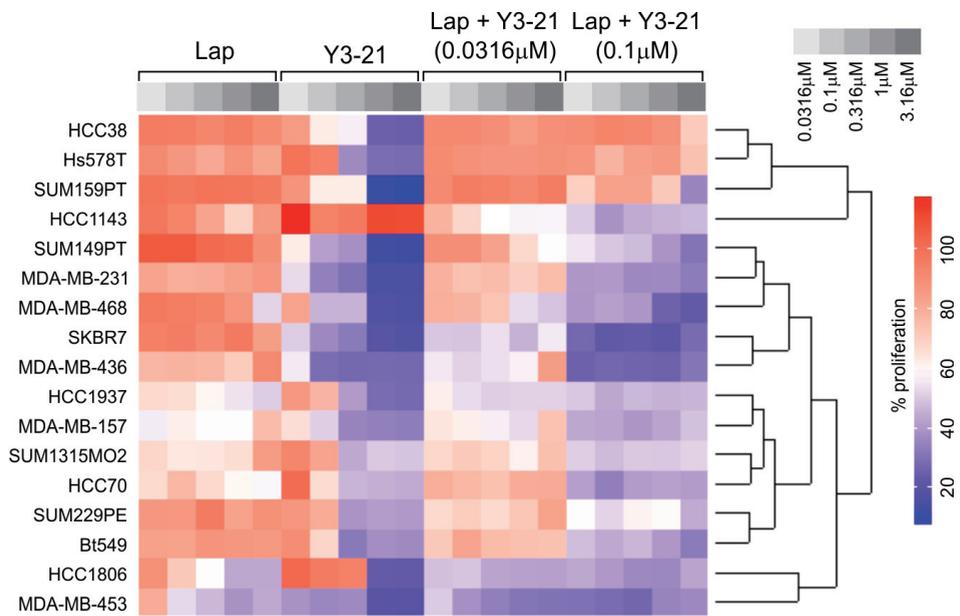
Supplementary Figure S2. A. Combining CDK9 inhibitor Y3-21 (0.0316 or 0.1 µM) with EGFR inhibitor lapatinib in concentration range (0.0316-3.16 µM) enhances proliferative inhibition in TNBC cell lines. Proliferation was evaluated using SRB assay after 4 days' treatment. Results shown as percentage proliferation normalised to DMSO control.

Supplementary Figure S3. CDK9 inhibitor I-73 and EGFR inhibitor lapatinib synergise to block growth factor-mediated networks (**A**) and MAPK/MEK downstream signalling (**B**). The colours of the nodes are as follows; red represents up-regulation, green represents down-regulation, and blue indicates inhibition. The colours of the lines indicating effects are as follows: blue represents inhibition, yellow indicates an inconsistent effect, whereas grey represents events lacking prediction. The heatmap in (**B**) shows the Log_2 fold change (FC) in expression of genes involved in MAPK/MEK-mediated signal transduction after treatment with lapatinib (3.16 μM), I-73 (0.1 μM) or lapatinib (3.16 μM) combined with I-73 (0.1 μM).